Molecular cloning of Porimin, a novel cell surface receptor mediating oncotic cell death

Fengrong Ma*, Chonghui Zhang*, K. V. S. Prasad†, Gordon J. Freeman‡, and Stuart F. Schlossman*§

*Division of Tumor Immunology and ‡Department of Adult Oncology, Dana–Farber Cancer Institute, Department of Medicine, Harvard Medical School, Boston, MA 02115; and †Department of Micro/Immunology, University of Illinois, Chicago, IL 60612

Contributed by Stuart F. Schlossman, June 26, 2001

Anti-Porimin (*P*ro-*o*ncosis *r*eceptor *i*nducing *m*embrane *in*jury) mAb mediates oncosis-like cell death in Jurkat cells. Porimin cDNA was isolated from a Jurkat cell cDNA library by COS cell-expression cloning. The 3,337-bp cDNA has an ORF of 567 bp, encoding a type I transmembrane protein of 189 amino acids. The extracellular domain of Porimin contains many *O*-linked and seven *N*-linked glycosylation sites that define it as a new member of the mucin family. COS7 and 293 cells transiently transfected with Porimin cDNA were specifically recognized by anti-Porimin Ab in cell staining and immunoblotting experiments. When expressed in Jurkat cells, a His-tagged Porimin cDNA construct resulted in the generation of a specific 110-kDa-size protein that matched the molecular mass of the endogenous Porimin protein. Crosslinking of the Porimin receptor expressed on COS7 transfectants resulted in the loss of cell membrane integrity and cell death as measured by the leakage of intracellular lactate dehydrogenase. Both COS7 and 293 cells expressing transfected Porimin at a relatively high level lost their ability to adhere to culture dishes, suggesting a role for Porimin in cell adhesion. The *Porimin* gene was mapped to human chromosome 11q22.1 and is composed of four exons spanning 133 kb of genomic DNA.

The importance of cell death is demonstrated by the fact that dysregulation of cell death can lead to cancer, developmental abnormalities, and autoimmune disorders. Both cell proliferation/differentiation and cell death are equally important for maintaining proper homeostasis. Tremendous progress in our understanding of apoptosis has been made following the molecular cloning of cell death receptors, including CD95 (Fas/Apo-1) and tumor necrosis factor receptor 1 (TNFR1). Engagements of these receptors by their ligands or specific Abs are known to initiate the activation of a cysteine protease cascade and subsequent cleavage of various cellular components resulting in cell death. Cells undergoing apoptosis are characterized by morphologic changes, including cellular shrinkage, multiple buds and protrusions, and nuclear chromatin condensation, ultimately leading to DNA fragmentation (1–3).

Another less well known form of cell death is oncosis. A number of noxious stimuli and ischemia are known to lead to cell death with morphological changes distinct from apoptosis. Necrosis is often used to describe cell death lacking the characteristics of apoptosis. However, necrosis does not describe a pathway of cell death but refers to the intracellular degradative reactions occurring after the death of individual cells within a living organism by any mechanism, including apoptosis (4). Oncosis, a term derived from "onkos" (meaning swelling), was first used in 1910 to describe ischemic cell death in osteocytes, and was reintroduced recently to describe a form of cell death distinct from apoptosis (5). Oncotic cells are characterized by cell swelling, organelle swelling, vacuolization, and increased membrane permeability. Oncosis usually occurs rapidly after application of the injury, with early changes resulting in alterations in cell shape and volume. In monolayer cell culture, oncotic cells form cytoplasmic blebs and chromatin clumps, followed by cells pulling apart, rounding up, and detaching from the substrate (6). Oncotic cell death has been documented in human macrophages infected with virulent *Shigella flexneri* (7), in murine B16 melanoma cells treated *in vivo* with cyclophosphamide (8), in human peripheral blood lymphocytes treated with a high dose of staphylococcal toxin (9), or in RE2 Ab-mediated cell death of murine cells (10). The molecular and biochemical mechanisms underlying oncosis are still unclear. Some believe that oncosis is a result of a failure of the ionic pumps in the plasma membrane and decreased levels of cellular ATP (11). More recently, phospholipase A_2 has been documented to be involved in the process of cell membrane injury and membrane structural changes (12, 13).

We previously reported the generation and characterization of anti-Porimin mAb (IgM isotype). Crosslinking with anti-Porimin mAb induced Jurkat cell membrane injury followed by cell death. Anti-Porimin Ab defined a 110-kDa cell surface structure distinct from cell receptors known to induce apoptosis both in its cellular expression and functional characterization. Cell death trigged by anti-Porimin Ab was preceded by cell aggregation, formation of plasma membrane pores, and the appearance of membrane blebs. These cells show neither DNA fragmentation nor apoptotic bodies, but display lethal damage of the cell membrane. The dying cells were distinct from complement-dependent cytolysis or complement-independent apoptosis but manifested features similar to oncosis (14).

In this study, we describe the isolation of the cDNA encoding Porimin by expression cloning with anti-Porimin Ab. The Porimin cDNA encodes a type I transmembrane protein with extensive *O*- and *N*-linked glycosylation sites characteristic of a mucin. Engagement of Porimin protein expressed on COS7 cell transfectants by anti-Porimin Ab resulted in the loss of membrane integrity and cell death as measured by the leakage of intracellular lactate dehydrogenase (LDH) from the damaged cells.

Materials and Methods

Abs and Reagents. Monoclonal anti-Porimin Ab was generated and characterized as described (14, 15). Affinity-purified goat anti-mouse Ig-FITC-conjugated and goat anti-mouse Ig-peroxidase-conjugated Abs were purchased from Jackson ImmunoResearch. Mouse IgM (MsIgM) was obtained from Coulter. All other chemicals were obtained from Sigma unless otherwise indicated.

Construction of Jurkat T Lymphocyte cDNA Library. The cDNA library was constructed from Jurkat cell mRNA by using oligo(dT) and random priming. Double-stranded (ds) cDNA (dscDNA) was ligated into the pAXEF mammalian expression

Abbreviations: LDH, lactate dehydrogenase; GFP, green fluorescent protein.

Data deposition: The sequence reported in this paper has been deposited in the GenBank database (accession no. AY008283).

§To whom reprint requests should be addressed. E-mail: stuart_schlossman@dfci.harvard.edu.

The publication costs of this article were defrayed in part by page charge payment. This article must therefore be hereby marked "*advertisement*" in accordance with 18 U.S.C. §1734 solely to indicate this fact.

vector (16) and electroporated into *Escherichia coli* DH10B/P3. The resulting cDNA clones were amplified by growth in liquid culture, and plasmid DNA was prepared by cesium chloride-ethidium bromide gradient centrifugation procedure (17).

Library Screening by Expression Cloning. Library screening was carried out by expression cloning according to the method developed by Seed and Aruffo (17). The Jurkat cell cDNA library was transfected into COS cells by using DEAE-Dextran as a facilitator. Cells expressing cDNA encoding the Porimin antigen were recovered 48 h after transfection by incubation with anti-Porimin mAb at 4°C for 1 h, followed by panning on plastic dishes coated with goat anti-mouse IgM Abs. Episomal DNA was recovered from the panned cells by the Hirt procedure and electroporated into *E. coli* DH10B/P3. Spheroplast fusion was used to reintroduce the plasmids into COS cells for subsequent rounds of expression and panning for enrichment of positive clones. After the third round of panning, individual plasmids were transfected into COS cells followed by indirect immunofluorescence staining with anti-Porimin Ab. Positive cDNA inserts were sequenced.

Northern Blot and Multitissue Expression-Array Analysis. A human multitissue mRNA Northern blot membrane and a multitissue expression-array membrane (CLONTECH) were hybridized according to the manufacturer's directions. Briefly, the 5′ terminal 1.3-kb *Xba* Porimin cDNA fragment was labeled with [α-^{32}P]dCTP by random priming (GIBCO/BRL) and purified by Sephadex G-25 column chromatography. The blot was first subjected to prehybridization at 65°C for 30 min followed by hybridization at 65°C with the radiolabeled probe for 6 h. After extensive washing, the blot was exposed to x-ray film at −70°C for varying lengths of time.

Molecular Cloning. The Porimin-green fluorescent protein (GFP) fusion construct in pEF4 mammalian vector was constructed by ligating the fragment encoding the ORF of Porimin in-frame with the fragment encoding GFP amplified by PCR, using 5′-dATGCGGATCCTCTAGAATGGCTAGCAAAGGAGA-AGAA-3′ and 5′-dGGAATCTAGATTTGTAGAGCTCATC-CATGCC-3′ as primers, and cloned into vector pEF$_4$/V5-His. Porimin cDNA with His$_6$ tag was constructed by ligating the Porimin cDNA ORF in-frame in vector pEF$_4$/V5-His. The cytoplasmic tail deletion form of *Porimin* was cloned by PCR amplification from the N terminus of the *Porimin* ORF to the lysine residue after the transmembrane domain and cloned into pEF$_4$ vector. Plasmids of reconstructed clones were selected and verified by sequencing.

Western Blot Analysis. Eukaryotic cell transfection of plasmid DNA was carried out by using SuperFect transfection reagent (Qiagen, Chatsworth, CA) according to the manufacturer's directions. Transiently transfected cells were lysed in 1% Triton lysis buffer at different time points. Whole-cell lysates were diluted in reducing SDS/PAGE sample buffer, and electrophoresis was carried out by using a 10% (vol/vol) SDS/PAGE gel. Proteins were transferred to nitrocellulose membrane (Bio-Rad). The filter was blocked and blotted with primary Ab followed by peroxidase-conjugated isotype-matched goat anti-mouse Ab. Protein bands were visualized with the enhanced chemiluminescence (ECL) system (Amersham Pharmacia).

Indirect Cell Staining and Flow Cytometry Analysis. Cells were transfected with plasmids by using SuperFect transfection reagent. At different times posttransfection, cells were suspended in 0.5 mM EDTA in PBS and blocked with 2% BSA/PBS. Then cells were incubated with primary Ab and FITC-conjugated second Ab on ice. After washing, cells were resuspended in 1 ml of fix buffer (0.5% formaldehyde in PBS) and subjected to flow cytometry analysis.

LDH Releasing Assay. Cells were transiently transfected with Porimin cDNA, and 24 h posttransfection the cells were suspended by trypsinization, seeded into 96-well plates at 1.0×10^4cells per well, and incubated overnight. After washing the wells with PBS and adding fresh medium, anti-Porimin Ab and control IgM Ab were added to the cells at different time intervals, and cells were incubated further at 37°C. Equal amounts of supernatants were withdrawn at the same time after incubation and LDH activity was determined by using the cytotoxicity detection kit (Roche Molecular Biochemicals) according to the manufacturer's directions.

Results

Isolation of a cDNA Encoding Porimin. The Jurkat T cell line highly expresses Porimin antigen (14). A Jurkat cell cDNA expression library was constructed and transfected into COS7 cells followed by expression cloning with anti-Porimin Ab. Three cDNA clones were isolated after three cycles of expression and enrichment through panning. Transfection of each of these three clones into COS7 cells resulted in the acquisition of reactivity with Porimin mAb. Each of the plasmids contained a single cDNA insert of ≈3.3 kb. DNA sequencing demonstrated that the three positive clones have the same ORF but slightly different lengths of 3′ untranslated region. Anti-Porimin Ab can also recognize the protein encoded by Porimin cDNA when expressed on other cell lines such as 293 and HeLa cells. The full-length cDNA comprised 3,337 bp, which terminated in a poly(A)$^+$ tail (GenBank accession no. AY008283). The ORF encodes a type I membrane protein of 189 amino acids (Fig. 1*A*). There is a signal peptide at its N-terminal, which is predicted to be cleaved between Ala-31 and Met-32 (SIGNALP prediction; Neural Networks; ref. 18). The predicted mature Porimin peptide consists of an extracellular domain (118 amino acids), a hydrophobic transmembrane domain (20 amino acids), and a cytoplasmic tail (20 amino acids). There are seven potential sites (Asn-X-Ser/Thr) for the attachment of *N*-linked carbohydrate. Almost 50% of the extracellular domain consists of threonine and serine, among which 35 residues are predicted to be *O*-glycosylated (NETOGLYC 2.0 prediction software), suggesting that Porimin is a new member of the membrane mucin family. There is a lysosome/endosome targeting motif, YXXϕ (where ϕ is a bulky hydrophobic amino acid), in the intracellular domain of Porimin. Double indirect immunostaining with anti-Porimin Ab and anti-Lamp1 antiserum in 293 cell transfectants demonstrated partial colocalization of these two proteins, suggesting that the YXXϕ motif could be functional (data not shown). A BLAST search of GenBank showed that Porimin cDNA shares 35% identity and 50% similarity with a gene product from *Drosophila melanogaster* (accession no. AE003551); 29% identity with CD164 (accession no. AB028895), a sialomucin highly expressed on CD34$^+$ hematopoietic progenitor cells; and 29% identity with endolyn (accession no. AJ238574), a recently cloned mucin-like type I membrane protein (19). A BLAST search of the human genome mapped the *Porimin* gene to chromosome 11q22.1. The *Porimin* gene consists of 4 exons covering 133 kb of genomic DNA (Fig. 1*B*). Interestingly, the genomic location of *Porimin* is overlapping with a family of apoptosis inhibitory proteins including IAP, MIHA, MIHB, and MIHC (20). The chromosome translocation t(11;18)(q21;q21), found in mucosa-associated lymphoid tissue (MALT) lymphomas, is closely adjacent to the *Porimin* gene (21).

Tissue Distribution. Northern blot analysis reveals the presence of Porimin mRNA (≈3.3 kb) in all tissues tested. Apart from the 3.3-kb band corresponding to Porimin, an mRNA around 1.35 kb

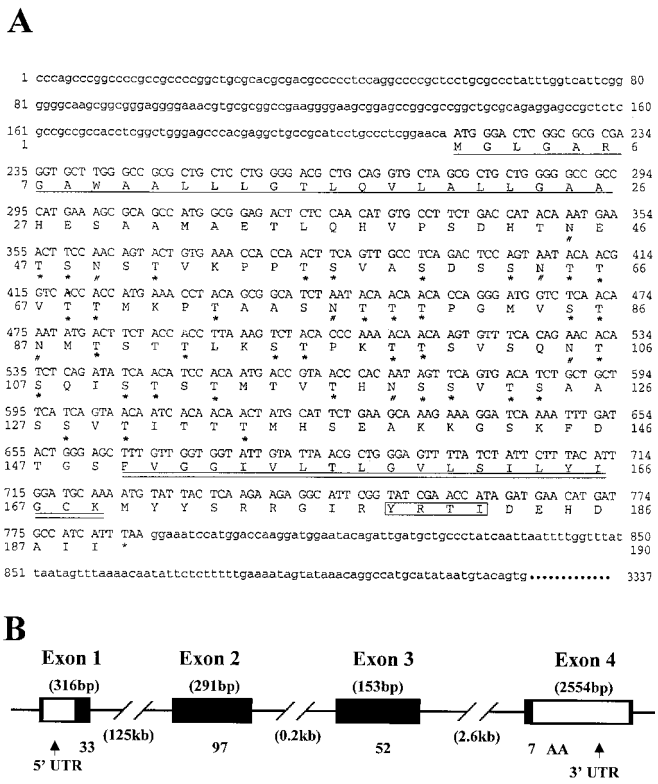

Fig. 1. Nucleotide and predicted protein sequence of *Porimin*. Porimin cDNA was cloned by means of expression cloning with anti-Porimin Ab. Three independent positive clones were obtained after three rounds of panning. The resulting cDNA sequence is 3,337 bp with an ORF encoding a 189-aa-long protein (GenBank accession no. AY008283). (*A*) The partial sequence of Porimin cDNA with its full coding peptide sequence is shown. The putative signal peptide is underlined. Potential *N*- and *O*-linked glycosylation sites are indicated by # and *, respectively. The putative transmembrane domain is double-underlined. (*B*) By using full-length Porimin cDNA for a BLAST search in the human genomic database, the Porimin cDNA sequence was found in 4 exons in chromosome 11q22.1 with 99.9% identity spanning 133 kb of genomic DNA.

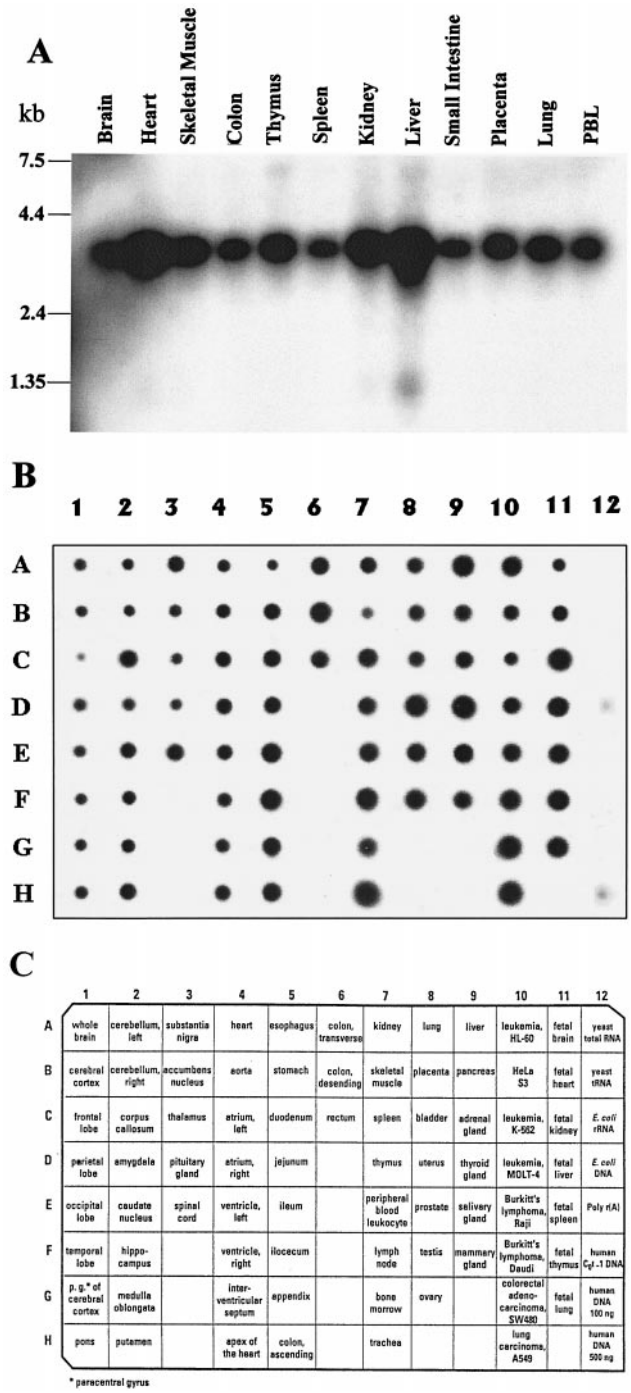

Fig. 2. Porimin mRNA expression in human tissues. The 5′-terminal 1.3-kb *Xba*I cDNA fragment of *Porimin* was labeled with [α-^{32}P]dCTP as a probe. Hybridization was carried out according to manufacturer's directions. (*A*) Northern blot analysis of Porimin expression by using a human 12-lane mRNA blot (human 12-lane multiple-tissue Northern blot from CLONTECH). (*B*) Expression of Porimin mRNA in 76 selected human tissues and tumor cell lines was detected by dot hybridization with Porimin probe and is shown in columns 1–11. Column 12 contains 8 negative control RNA. (*C*) The corresponding identities of each tissue present on the dot blot are shown.

in human liver also weakly hybridized to the Porimin probe (Fig. 2*A*). Porimin seems to be ubiquitously expressed in human tissues according to multiple tissue expression array hybridization analysis (Fig. 2*B*). Seven tissues and cell lines had comparable and relatively high levels of Porimin mRNA, including trachea (H7), fetal kidney (C11), uterus (D8), thyroid gland (D9), adult liver (A9), and two tumor cell lines, colorectal adenocarcinoma SW480 (G10) and lung carcinoma A549 (H10). Fetal tissues have high levels of Porimin expression, including fetal kidney, liver, spleen, thymus, and lung. Gastrointestinal system analysis reveals abundant Porimin expression, excluding esophagus (columns 5 and 6, Fig. 2*B*). The only tissue that does not express Porimin is ovary (G8). The eight dots in the negative control column (column 12) did not hybridize with the probe. To exclude the possibility that the 1.3-kb Porimin cDNA probe we used crossreacted with another mRNA, the RNA blots were reprobed with Porimin coding-specific cDNA probe. Similar hybridization results were obtained by using these two probes (data not shown).

Porimin Protein Molecular Mass Varies in Different Cell Lines. Porimin cDNA was transiently transfected into 293, COS7, and HeLa cells. Whole-cell lysates of the above transfectants along with Jurkat cells were used for Western blot analysis with anti-Porimin Ab. As shown in Fig. 3*A*, the molecular mass of expressed Porimin varied depending on the cell type, ranging from 55 to 80 kDa, compared with the endogenous molecular mass of 110 kDa in Jurkat cells. The variation in protein size led to the question whether the Porimin cDNA indeed coded for the structure on Jurkat cells that is recognized by the Porimin mAb.

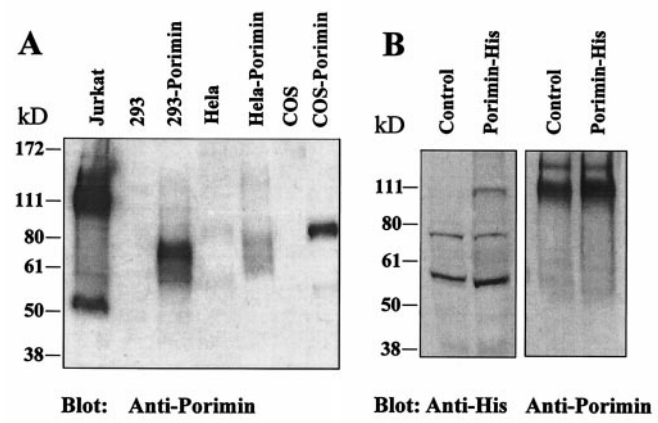

Fig. 3. Biochemical characterization of the cloned Porimin cDNA. Molecular mass of Porimin cDNA-derived protein expressed in different cell lines was determined by Western blot analysis. (*A*) Full-length Porimin cDNA cloned in mammalian expression vector pAXEF was transiently transfected into 293, COS7, and HeLa cells, and transfectants were lysed 29 h posttransfection. Cell lysates of 293, COS7, and HeLa cells, with or without Porimin cDNA transfection, together with lysates of Jurkat cells were electrophoresed and transferred onto nitrocellulose membrane. Membranes were blotted with anti-Porimin Ab, and the resulting proteins were detected by chemiluminescence assay. (*B*) To confirm the molecular mass of Porimin cDNA-derived protein expressed in Jurkat cells, a His-tagged Porimin cDNA was cloned into pEF4 vector and electroporated into Jurkat cells. Cell lysates of both Jurkat cells and Jurkat transfectants were electrophoresed and transferred onto nitrocellulose. *B Left* represents the resulting protein with anti-His Ab blotting. The same blot was stripped and reprobed with anti-Porimin Ab and is shown (*B Right*) for the endogenous Porimin protein in Jurkat cells.

To verify the exogenously expressed Porimin in Jurkat cells, a His tag was added at the C terminus of the Porimin cDNA. Lysates of Jurkat cells and Jurkat cells transfected with the Porimin-His cDNA were sequentially blotted with anti-His and anti-Porimin mAb. As shown in Fig. 3*B*, a 110-kDa band protein was specifically detected by anti-His mAb in lysates of Porimin cDNA transfectants, which exactly matched the molecular mass of endogenous Porimin in Jurkat cells. A similar result was obtained by using an HA-tagged Porimin construct (data not shown), thus clearly confirming that the cDNA in question does in fact code for Porimin. The polypeptide backbone of Porimin is predicted to be 19 kDa, but the actual molecular mass of Porimin in different cells is increased by approximately 3–5-fold. The difference in the size of the Porimin protein in the different cell types presumably reflects differences in the number and complexity of glycosylation.

Anti-Porimin Antibody Mediates Cell Membrane Injury and Cell Death of COS7 Transfectants. Our previous studies have shown that Jurkat cells when treated with anti-Porimin Ab undergo oncosis-like cell death (14). Therefore, we investigated whether expression of the Porimin cDNA in other cells rendered them susceptible to Porimin-mediated cell death. COS7 cells were transiently transfected with plasmids consisting of vector control, Porimin-ΔCyt (cytoplasmic tail deletion form of Porimin), and Porimin cDNA (full length). Transfection efficiency was determined by flow cytometric analysis to be 19–24% (Fig. 4*A*). These transfected cells were incubated with anti-Porimin Ab and assayed for cell membrane injury by measuring LDH activity leaked from damaged cells. Before incubation with mAbs, cells in 96-well plates were washed to get rid of both dead cells and accumulated LDH activity from overnight culture. As shown in Fig. 4*B*, cell death as measured by LDH leakage was observed 30 min after anti-Porimin Ab treatment in cells transfected with full-length Porimin cDNA, but not with Porimin-ΔCyt or vector control. Cell death increased to 12% after 2 h of anti-Porimin Ab treatment. Cell death in control groups was low. Given that the transfection efficiency of Porimin was 23% on average, nearly 50% of Porimin-expressing cells were killed by anti-Porimin mAb treatment. The accompanying morphological changes were consistent with observed cell death based on LDH leakage (Fig. 4*C*). Our data also suggested that the cytoplasmic tail of Porimin was essential for mediating cell death. The expression of Porimin protein in COS7 cells seems to be toxic, which is reflected in an inability to achieve a high transfection efficiency of Porimin cDNA into COS7 cells, whereas that the transfection efficiency of pEGFP vector control could reach 80%. Many of the transfected cells with relatively high Porimin protein expression died before we could undertake further experiments. Attempts to generate stable transfectants of COS7 cells were unsuccessful but showed initial expression of Porimin that was lost with further cell culture (data not shown).

Porimin-Transfected Adherent Cells Detach and Change Morphology. A GFP tag was added at the C terminus of Porimin cDNA, and the Porimin-GFP fusion protein construct was transfected into COS7 and 293 cells. As shown in Fig. 5, cells that highly expressed Porimin-GFP detach from the plastic surface and round up, compared with neighboring cells lacking Porimin-GFP expression.

Discussion

We previously reported a mAb, anti-Porimin, which caused Jurkat cells to undergo a unique form of cell death, termed oncosis. Anti-Porimin-triggered cell death showed no evidence of DNA fragmentation or formation of apoptotic bodies but did, however, rapidly show plasma-membrane injury followed by cell death (14). Anti-Porimin mAb defined a 110-kDa surface structure on Jurkat cells, a human T leukemia cell line. In this study, we report the isolation of Porimin cDNA by means of COS cell-expression cloning by using anti-Porimin Ab. The Porimin cDNA encodes a type I transmembrane mucin. Crosslinking of Porimin on transient COS transfectants caused cell-membrane injury and death as measured by LDH release.

Transiently expressed Porimin cDNA in 293 and COS7 cells can be recognized by anti-Porimin Ab either by cell surface staining or Western blot analysis. GFP-tagged Porimin protein expression on 293 cells was coincident with anti-Porimin Ab staining (data not shown). His- and HA-tagged Porimin cDNA constructs encode a 110-kDa protein in Jurkat cells, identical to the size of endogenous Porimin. Porimin cDNA encoded 55–80-kDa structures in other cell types, indicating heterogeneity in the level of posttranslational modification.

The Porimin mRNA was expressed ubiquitously in human tissues, which is in sharp contrast to the restricted expression of the antigenic determinant recognized by anti-Porimin mAb. Many cell lines expressed Porimin mRNA but not the cell surface antigen. We found that de-glycosylation of affinity purified Porimin protein from Jurkat cells resulted in loss of reactivity with the anti-Porimin mAb (data not shown). Our data suggest that anti-Porimin mAb reacts in part or completely with a carbohydrate epitope. We transfected Porimin cDNA into several cell lines and found that transfected Porimin could be recognized by anti-Porimin mAb in some cell lines such as 293 and COS7 but not others like MCF7. Alternatively, translation of the Porimin mRNA may be tightly regulated or a glycosyltransferase necessary for the Porimin epitope may be narrowly expressed.

The biological event that initiates Porimin-mediated cell death is not known. Porimin may bind to a receptor that mediates its function. Whether the anti-Porimin epitope is required for this interaction or whether other parts of the Porimin structure mediate binding to such a receptor remains to be determined.

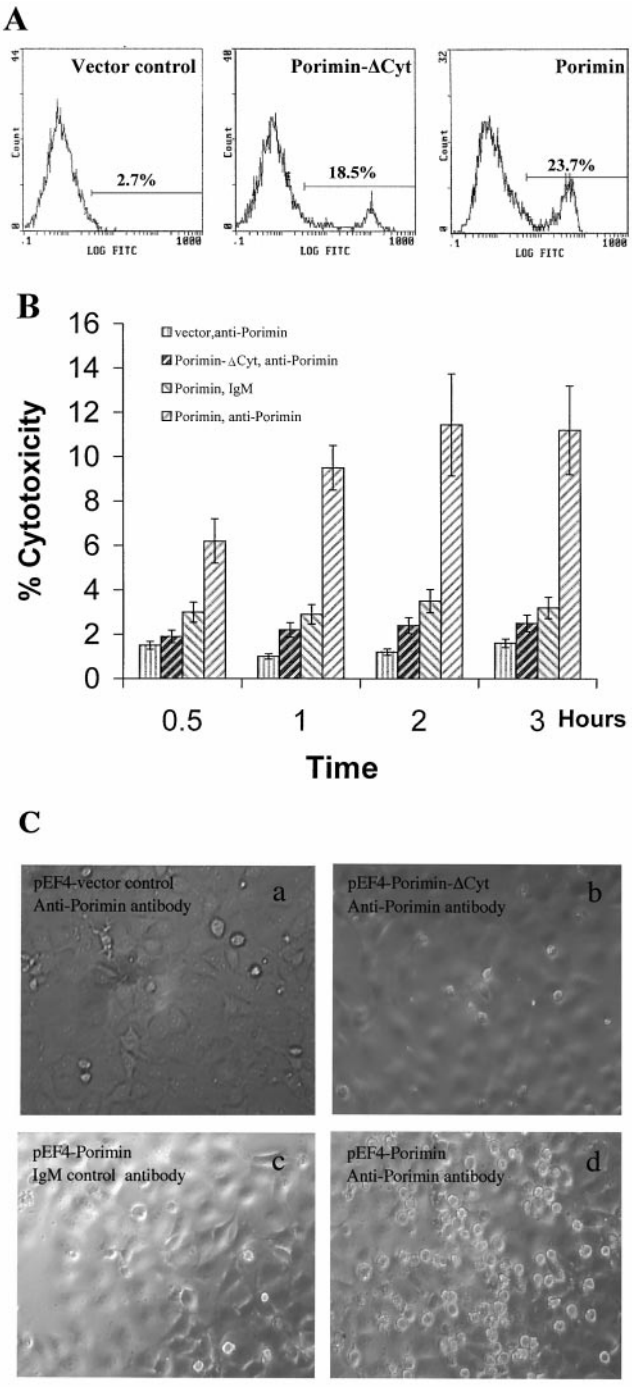

Fig. 4. Anti-Porimin mAb-mediated cell membrane injury and cell death of COS7 cell transfectant with Porimin. COS7 cells were transiently transfected with plasmids consisting of vector control, Porimin-ΔCyt (a cytoplasmic tail deletion form of Porimin), and Porimin cDNA (full length). (*A*) Two days later, cells were harvested and indirectly immunostained with anti-Porimin Ab or control IgM Ab, and transfection efficiency was demonstrated by flow cytometric analysis. *A Left*, vector control; *A Center*, Porimin-ΔCyt cDNA; *A Right*, Porimin cDNA. (*B* and *C*) Cells were trypsinized 24 h posttransfection and seeded into 96-well plates at 1.0×10^4 cells per well for overnight incubation. After washing the wells with PBS and adding fresh medium, Abs were added to the cells at different times for further incubation. After 0.5, 1, 2, and 3 h of Ab treatment, the same amount of supernatant was withdrawn from each well. Cytotoxicity of different transfectants with anti-Porimin Ab and control Ab treatment was measured by the LDH releasing assay (*Materials and Methods*). *C* shows typical cell morphologic changes after 2 h of Ab treatment as demonstrated by phase contrast imaging. These data are representative of five independent experiments.

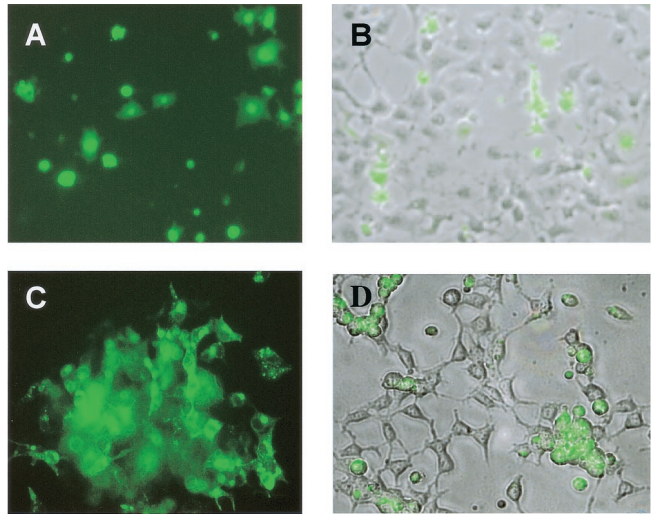

Fig. 5. Expression of Porimin causes loss of cell adhesion. A GFP tag was added at the C terminus of Porimin cDNA, and the Porimin-GFP fusion protein construct was transfected into COS7 and 293 cells. Images were taken 48 h posttransfection. *A* and *B* represent COS7 transfectant and *C* and *D* represent 293 transfectant. Images *A* and *C* were taken under fluorescence view. *B* and *D* were superimposed on fluorescence images with the corresponding phase contrast.

We showed in this study that crosslinking of Porimin in COS7 transfectants could mediate cell-membrane injury and cell death. COS7 transfectants lost cell-membrane integrity as early as 30 min after anti-Porimin mAb treatment as shown by an LDH leakage assay, which further supports our previous observation that Porimin mAb mediates cell death through injury of the cell membrane in Jurkat cells. That engagement of the cytoplasmic tail deletion form of Porimin with anti-Porimin Ab did not result in cell death clearly suggests an indispensable role for the cytoplasmic tail in this cell-injury process. The 20-aa long cytoplasmic tail of Porimin lacks distinct motifs, thus suggesting that a novel signal pathway is initiated. The cytoplasmic tail of Porimin contains three tyrosines and a protein kinase C consensus recognition site (SRR), but additional studies will be required to determine whether they are of functional significance in this cell death pathway.

We also noticed that the expression of Porimin protein in COS7 cells caused profound toxicity in these cells and overexpression led to cell death. Many COS7 cells transfected with Porimin showed multiple morphological changes and formation of blebs on the cell surface. Cell-membrane blebbing has been observed at an early stage as a result of toxic injury in many cell types, including those of liver, kidney, and heart. Blebbing is followed by increased membrane permeability, loss of cellular contents, and cell death (22). Overexpression of the Porimin protein may trigger a cell-injury pathway in COS7 cells once the accumulation of Porimin protein reaches a sufficiently high level. In contrast, cell death was not induced in 293 cell transfectants by anti-Porimin Ab. It is possible that 293 cells do not have all of the elements required for Porimin-mediated cell death. Alternatively, 293 cells might express an antagonist of the Porimin-mediated cell death pathway. Such a possibility would be consistent with studies of programmed cell death. In the case of apoptosis, it has been observed that some cells are sensitive to apoptosis signaling, whereas others are resistant even though they express the same cell death receptor and receive the same death signal (1).

Porimin is a highly glycosylated protein that can be classified as a member of the cell membrane-associated mucin family. The

various members of the mucin family have a relatively high content of threonine and serine residues comprising 20–55% of the amino acid composition, but share limited homology. The extracellular region of Porimin contains 50% threonine and serine residues, which allows a high density of *O*-linked glycosylation. In addition, Porimin contains seven potential sites for *N*-linked glycosylation.

Mucin family members have diverse functions. Loss of cell adhesion is associated with the expression of many cell surface mucins, such as MUC1 and CD43 (23, 24). Porimin transfectants showed a loss of cell adhesion. A large proportion of either 293 or COS7 cell transfectants detached from their supporting dishes after Porimin protein expression (Fig. 5 *B* and *D*). Membrane mucins have been shown to exhibit both anti- and proadhesive properties. The dense array of *O*-linked highly negatively charged side chains in membrane mucins gives them a rigid and extended structure, which makes them long enough to extend above the glycocalyx (25). By virtue of their negative charge and extended configuration, membrane mucins act as a repulsive barrier around a cell surface. However, when an opposing cell has a specific receptor for the membrane mucin, adhesion surpasses repulsion. The two-faceted adhesion and antiadhesion function of membrane mucins may have a profound role in hematopoietic cells. It might allow cells to move freely in the blood stream or tissues and also permit their targeting to specific areas when needed.

Porimin is a membrane mucin that mediates cell death. Although mucins mainly affect cell adhesion and ligand binding, several membrane mucins have also been documented to trigger cell death or inhibition of cell proliferation, such as CD43 (leukosialin, sialophorin), CD162 (PSGL-1), and CD164 (MGC-24v; refs. 26–29). Further studies on Porimin should provide more information on the relationship between this membrane-associated mucin and cell death.

In summary, we cloned Porimin cDNA and found it to encode a membrane mucin that mediated oncosis-like cell death in Jurkat cells. Expression of Porimin cDNA in COS7 cells initiated not only morphological changes but also mediated cell-membrane injury and cell death after anti-Porimin Ab treatment. The molecular and biochemical mechanisms underlying oncosis are still largely unknown. The molecular cloning of a receptor that mediates oncosis-like cell death should permit the further understanding of this novel nonapoptotic cell-death pathway.

We thank J. S. Duke-Cohan for his helpful comments and Dr. Q. Medley for critical reading of the manuscript. This work was supported by National Institutes of Health Grants AI12069 and CA84500.

1. Smith, C. A., Farrah, T. & Goodwin, R. G. (1994) *Cell* **76,** 959–962.
2. Trauth, B. C., Klas, C., Peters, A. M. J., Matzku, S., Moller, P., Falk, W., Debatin, K.-M. & Krammer, P. H. (1989) *Science* **245,** 301–305.
3. Tartaglia, L. A., Rothe, M., Hu, Y.-F. & Goeddel, D. V. (1993) *Cell* **73,** 213–216.
4. Majno, G. & Joris, I. (1995) *Am. J. Pathol.* **146,** 3–15.
5. Trump, B. F., Berezesky, I. K., Chang, S. H. & Phelps, P. C. (1997) *Toxicol. Pathol.* **25,** 82–88.
6. Phelps, P. C., Smith, M. W. & Trump, B. F. (1989) *Lab. Invest.* **60,** 630–642.
7. Fernandez-Prada, C. M., Hoover, D. L., Tall, B. D. & Venkatesan, M. M. (1997) *Infect. Immun.* **65,** 1486–1496.
8. Kuwashima, Y. (1996) *Anticancer Res.* **16,** 2997–3000.
9. Jonas, D., Walev, I., Berger, T., Liebertrau, M., Palmer, M. & Bhakdi, S. (1994) *Infect. Immun.* **62,** 1304–1312.
10. Matsuoka, S., Asano, Y., Sano, K., Kishimoto, H., Yamashita, I., Yorifuji, H., Utsuyama, M., Hirokawa, K. & Tada, T. (1995) *J. Exp. Med.* **181,** 2007–2015.
11. Eguchi, Y., Shimizu, S. & Tsujimoto, Y. (1997) *Cancer Res.* **57,** 1835–1840.
12. Cummings, B. S., McHowat, J. & Schnellmann, R. G. (2000) *J. Pharmacol. Exp. Ther.* **294,** 793–799.
13. Sapirstein, A. & Bonventre, J. V. (2000) *Biochim. Biophys. Acta.* **1488,** 139–148.
14. Zhang, C. H., Xu, Y. H., Gu, J. J. & Schlossman, S. F. (1998) *Proc. Natl. Acad. Sci. USA* **95,** 6290–6295.
15. Zhang, C., Ao, Z., Seth, A. & Schlossman, S. F. (1996) *J. Immunol.* **157,** 3980–3987.
16. Freeman, G. J., Cardoso, A. A., Boussiotis, V. A., Anumanthan, A., Groves, R. W., Kupper, T. S., Clark, E. A. & Nadler, L. M. J. (1998) *Immunology* **161,** 2708–2715.
17. Seed, B. & Aruffo, A. (1987) *Proc. Natl. Acad. Sci. USA* **84,** 3365–3369.
18. Nielsen, H., Engelbrecht, J., Brunak, S. & von Heijne, G. (1997) *Protein Eng.* **10,** 1–6.
19. Ihrke, G., Gray, S. R. & Luzio, J. P. (2000) *Biochem. J.* **345,** 287–296.
20. Liston, O., Roy, N., Tamai, K., Lefebvre, C., Baird, S., Cherton-Horvat, G., Farahani, R., McLean, M., Ikeda, J. E., MacKenzie, A. & Korneluk, R. G. (1996) *Nature (London)* **379,** 349–353.
21. Dierlamm, J., Bacens, M., Wlodarska, I., Stefanova-Ouzounova, M., Hernandez, J. M., Hossfeld, D. K., De Wolf-Peeters, C., Hagemeijer, A., Berghe, H. & Marynen, P. (1999) *Blood* **93,** 3601–3609.
22. Tee, L. B. G., Boobis, A. R, Huggett, A. C. & Davies, D. S. (1986) *Toxicol. Appl. Pharmacol.* **83,** 294–314.
23. Ostberg, J. R., Barth, R. K. & Frelinger, J. G. (1998) *Immunol. Today* **19,** 546–550.
24. Ligtenberg, M. J., Buijs, F., Vos, H. L. & Hilkens, J. (1992) *Cancer Res.* **52,** 2318–2324.
25. Shimizu, Y. & Shaw, S. (1993) *Nature (London)* **366,** 630–631.
26. Bazil, V., Brandt, J., Tsukamoto, A. & Hoffman, R. (1995) *Blood* **86,** 502–511.
27. Manjunath, N., Correa, M., Ardman, M. & Ardman, B. (1995) *Nature (London)* **377,** 535–538.
28. Levesque, J. P., Zannettino, A. C. W., Pudney, M., Niutta, S., Haylock, D. N., Snapp, K. R., Kansas, G. S., Berndt, M. C. & Simmons, P. J. (1999) *Immunity* **11,** 369–378.
29. Zammettino, A. C. W., Buhring, H. J., Niutta, S., Watt, S. M., Benton, M. A. & Simmons, P. J. (1998) *Blood* **92,** 2613–2628.